

## Examination of the relationship between the parameters of Barkhausen effect model and microstructure of magnetic materials

C. C. H. Lo, S. J. Lee, L. C. Kerdus, and D. C. Jiles

Citation: *J. Appl. Phys.* **91**, 7651 (2002); doi: 10.1063/1.1453312

View online: <http://dx.doi.org/10.1063/1.1453312>

View Table of Contents: <http://jap.aip.org/resource/1/JAPIAU/v91/i10>

Published by the [American Institute of Physics](http://www.aip.org).

---

### Related Articles

Piezoresponse force microscopy and vibrating sample magnetometer study of single phased Mn induced multiferroic BiFeO<sub>3</sub> thin film

*J. Appl. Phys.* **111**, 064110 (2012)

Tunable magnetocaloric effect near room temperature in La<sub>0.7-x</sub>Pr<sub>x</sub>Sr<sub>0.3</sub>MnO<sub>3</sub> (0.02 ≤ x ≤ 0.30) manganites

*J. Appl. Phys.* **111**, 063918 (2012)

Origin of magnetic properties and martensitic transformation of Ni-Mn-In magnetic shape memory alloys

*Appl. Phys. Lett.* **100**, 132402 (2012)

Ferromagnetic phase transition in zinc blende (Mn,Cr)S-layers grown by molecular beam epitaxy

*Appl. Phys. Lett.* **100**, 132405 (2012)

Magnetic properties and thermal stability of (Fe,Co)-Mo-B-P-Si metallic glasses

*J. Appl. Phys.* **111**, 063906 (2012)

---

### Additional information on *J. Appl. Phys.*

Journal Homepage: <http://jap.aip.org/>

Journal Information: [http://jap.aip.org/about/about\\_the\\_journal](http://jap.aip.org/about/about_the_journal)

Top downloads: [http://jap.aip.org/features/most\\_downloaded](http://jap.aip.org/features/most_downloaded)

Information for Authors: <http://jap.aip.org/authors>

## ADVERTISEMENT



**FIND THE NEEDLE IN THE  
HIRING HAYSTACK**

Post jobs and reach  
thousands of hard-to-find  
scientists with specific skills



<http://careers.physicstoday.org/post.cfm> **physicstoday** JOBS

# Examination of the relationship between the parameters of Barkhausen effect model and microstructure of magnetic materials

C. C. H. Lo, S. J. Lee, L. C. Kerdus, and D. C. Jiles  
 Center for Nondestructive Evaluation, Iowa State University, Ames, Iowa 50011

A relationship between the parameters of a hysteretic-stochastic process model of the Barkhausen effect (BE) and the microstructural features of a series of ferritic/pearlitic steel samples has been identified. The root-mean-square values and pulse height distributions of the experimental and modeled BE signals showed similar dependence on the pearlite content. The correlation length parameter  $\xi$  of the model, which represents the range of interaction of domain walls with pinning sites, was found to obey  $\xi = AV_f D_f + BV_p D_p$  where  $V_f (V_p)$  and  $D_f (D_p)$  are the volume fraction and grain size of ferrite (pearlite). © 2002 American Institute of Physics.  
 [DOI: 10.1063/1.1453312]

## I. INTRODUCTION

A study of the relation between the Barkhausen effect (BE) and the structural features of ferrite/pearlite steels has been conducted. The nature of the BE signal, which results from discontinuous changes in magnetization of magnetic materials with a time dependent magnetic field, is closely related to the microstructure of the materials. The information obtained from BE measurements, when combined with a model description that can be used to interpret the measurement results, can be exploited to assess the microstructure of the magnetic materials. The stochastic process model of domain wall dynamics developed by Bertotti *et al.* (ABBM)<sup>1-3</sup> has provided a mathematical description of the intrinsically random nature of Barkhausen emissions. The model has recently been generalized to include magnetic hysteresis<sup>4,5</sup> so that the Barkhausen effect can be described over an entire hysteresis cycle.

In the hysteretic-stochastic process model of the Barkhausen effect the properties of BE signal are determined by two parameters,  $A$  and  $\xi$ , which, respectively, correspond to the intensity of the short-range fluctuation of the local pinning field experienced by a moving domain wall and the range of interaction of a domain wall with pinning sites.<sup>2</sup> The precise nature of the influence of the microstructure on BE can be elucidated by establishing links between the model parameters and the structural features of the magnetic materials. This approach has been adopted in previous studies on polycrystalline SiFe and AlSiFe ribbons in which  $\xi$  was found to be proportional to grain size.<sup>6,7</sup> No similar study on two-phase materials has yet been reported. The aim of the present study is to investigate the connection between the BE model parameters and the structure of ferritic/pearlitic steel through measurements and theoretical modeling of Barkhausen effects based on the hysteretic-stochastic process model of the Barkhausen effect.

## II. HYSTERETIC EXTENSION TO THE STOCHASTIC MODEL OF BARKHAUSEN EFFECT

According to the ABBM model of Barkhausen effect changes in magnetic flux  $\phi$  with time caused by a moving domain wall can be described by<sup>2</sup>

$$\frac{d\phi}{dt} + \frac{\phi - SI}{\tau} = -\frac{1}{\sigma G} \frac{dH_c}{dt}, \quad \tau = \sigma GS\mu, \quad (1)$$

where  $\mu$  is the permeability,  $\sigma$  is the electrical conductivity,  $S$  is the area of the domain wall, and  $G$  is a dimensionless coefficient.<sup>2</sup> The local coercive field  $H_c$  is governed by<sup>2</sup>

$$\frac{dH_c}{dI_{irr}} + \frac{S(H_c - \langle H_c \rangle)}{\xi} = \frac{dW}{dI_{irr}}, \quad (2)$$

where  $\xi$  represents the range of interaction of a domain wall with pinning sites. The function  $W (I_{irr})$  describes the Wiener-Lévy process<sup>2</sup> and has a zero mean but a finite variance which is proportional to the intensity of the local pinning field  $A$ , i.e.,

$$\langle dW \rangle = 0, \quad \langle |dW|^2 \rangle = 2AS dI_{irr}. \quad (3)$$

The assumptions used in the ABBM model limit its use to the cases where the rate of change of applied field with time is constant.<sup>2,3</sup> The model is also restricted to a small region of the hysteresis loop near the coercive point where the permeability is almost constant, and to soft magnetic materials where  $\mu/\mu_0 \gg 1$ .

These restrictions of the original ABBM model have been relieved by incorporating the theory of hysteresis developed by Jiles and Atherton.<sup>8</sup> According to the extended model Barkhausen jumps, which correspond to irreversible movements of the domain walls, occur only when there are irreversible changes in magnetization.<sup>4</sup> The BE signal voltage should therefore be expressed in terms of irreversible changes in magnetization  $I_{irr}$  instead of  $\phi$  as

$$\frac{dI_{irr}}{dt} = \frac{\chi'_{irr}}{\tau} \left( \frac{dH_a}{dt} - \frac{dH_c}{dt} \right) - \frac{I_{irr}}{\tau}, \quad (4)$$

where  $dH_a/dt$  is the rate of change of the applied field,  $\tau = \sigma GS\chi'_{irr}$  and  $\chi'_{irr}$  is the irreversible component of the differential susceptibility. The terms  $\chi'_{irr}$  and  $dH_a/dt$  are now functions of time rather than being constant as assumed in the original ABBM model. Also  $\tau$  is a function of the position on the hysteresis curve and is dependent on the magnetic history of the material. The extended model allows the BE signal to be calculated over an entire hysteresis cycle in which permeability varies with the applied field, thus provid-

TABLE I. Composition and structural parameters of the plain carbon steel samples.

Carbon content (wt. % C)	Volume fraction of ferrite $V_f$ (%)	Ferrite grain size $D_f$ ( $\mu\text{m}$ )	Volume fraction of pearlite $V_p$ (%)	Pearlite grain size $D_p$ ( $\mu\text{m}$ )
0.1	89	190	11	13
0.2	76	20	24	17
0.4	49	12	51	11
0.6	23	10	77	14
0.9	0	...	100	11

ing the mechanism for simulating the BE signal according to the variations in the hysteresis loop caused by external factors such as applied stresses, magnetizing field frequency, and amplitude.<sup>5</sup>

### III. RELATIONSHIP BETWEEN BE MODEL PARAMETERS AND MICROSTRUCTURE

For ferrite (bcc iron) the grain size is the most important structural factor that affects the magnetization reversal processes and the Barkhausen effect, since the grain boundaries act as both nucleation sites for reverse domains and pinning sites for domain walls. It has been shown in previous studies that the size of BE jumps in SiFe has a linear dependence on the grain size.<sup>6,7,9</sup> We therefore assume that in ferrite the domain walls interact with pinning sites over a range  $\xi$ , which is proportional to the ferrite grain size  $D_f$ . In ferritic/pearlitic steels the pearlite grains can strongly interfere with the movements of domain wall. It has been observed using Lorentz microscopy that domain walls can move freely through the ferrite, but are strongly pinned at the ferrite-pearlite boundaries.<sup>10</sup> Within a pearlite, grain domain walls lying parallel to cementite lamellae ( $\text{Fe}_3\text{C}$ ), which are planar magnetic inclusions, are strongly pinned, while those inclined at other angles to the cementite lamellae can readily move across the lamellae.<sup>10</sup> Therefore once the applied field is large enough to overcome the local pinning force at the cementite lamella, the domain wall will move across the pearlite grain and the adjacent ferrite grains until it is pinned again. The overall distance that the domain wall transverses is given by the product of the ferrite (pearlite) grain size and the number of ferrite (pearlite) grains it transverses. The latter is related to the volume fractions of the ferrite and pearlite. We therefore propose that the interaction range of the domain wall with pinning sites  $\xi$ , which is related to the displacement of the domain wall between pinning sites, is given by

$$\xi = AV_f D_f + BV_p D_p, \quad (5)$$

where  $V_f$  ( $V_p$ ) and  $D_f$  ( $D_p$ ) are the volume fraction and grain size of ferrite (pearlite), and the coefficients  $A$  and  $B$  are constants depending on the average number of grains that the domain wall transverses in the ferrite and pearlite phases.

### IV. PROCEDURES

A series of plain carbon steel samples with various carbon contents ranging from 0.1% to 0.9% C (wt. %) were

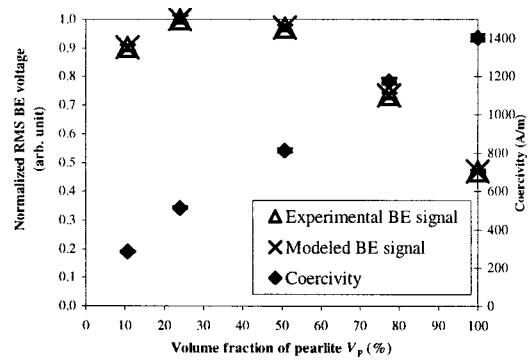


FIG. 1. Normalized rms values of the measured and modeled BE signal as a function of the volume fraction of pearlite  $V_p$ . The values were normalized with respect to the BE signal obtained from the 0.2% C sample. BE signals were simulated using  $A = 1 \times 10^4 \text{ A}^2 \text{ m}^{-2} \text{ Wb}^{-1}$ , and  $\xi = 8.75 \times 10^{-7}$ ,  $1 \times 10^{-7}$ ,  $4 \times 10^{-7}$ ,  $2.75 \times 10^{-7}$ , and  $1.5 \times 10^{-7} \text{ Wb}$  for the 0.1, 0.2, 0.4, 0.6, and 0.9% C samples.

used. It was found, using optical microscopy, that the 0.1% to 0.6% C samples have a ferritic/pearlitic structure, and the 0.9% C sample has a completely pearlitic structure. The volume fractions and grain sizes of the ferrite and pearlite grains of the samples are shown in Table I.

The samples were machined into rods of length 90 mm and diameter 6.4 mm for magnetic hysteresis and Barkhausen emission measurements. During the measurements a 2 Hz sinusoidal magnetizing field was applied to the sample. A Hall effect sensor was mounted on the sample surface to measure the surface field. The voltage signal induced across a flux coil encircling the sample was integrated to obtain magnetic induction. The flux coil signal was also filtered (pass band: 20–250 kHz) and amplified (voltage gain: 60 dB) to obtain the BE signal. The BE signal was then acquired by a computer for analysis using a recently developed software package<sup>11</sup> to obtain the rms value and pulse height distribution of the measured BE signal.

When simulating the BE signal using the extended model, experimental hysteresis loops were first analyzed using the theory of magnetic hysteresis<sup>12</sup> to obtain the model parameters that fully describe the hysteresis properties. The irreversible susceptibility  $\chi'_{\text{irr}}$  over a complete hysteresis cycle was then calculated based on the theory of magnetic hysteresis. The Barkhausen signal voltage as a function of time [i.e.,  $\dot{I}_{\text{irr}}(t)$ ] was calculated from  $\chi'_{\text{irr}}$  using Eqs. (3) and (4).

### V. RESULTS AND DISCUSSION

As shown in Fig. 1, the coercivity increases monotonically with pearlite content. This can be attributed to larger impedance to domain wall motion arising from strong domain wall pinning at the ferrite/pearlite interfaces and at the cementite lamellae inside the pearlite grains. The measured rms BE voltage first increased slightly to a maximum at  $V_p = 24\%$  and then decreased with increasing pearlite content. A possible explanation is that the total areas of ferrite-pearlite interfaces, which act as nucleation sites for reverse domains, would first increase with  $V_p$  and then decrease as  $V_p$  approaches 100%. An increase in the number of reverse domains, which can grow readily through domain wall motion, gives rise to a stronger BE signal and therefore accounts

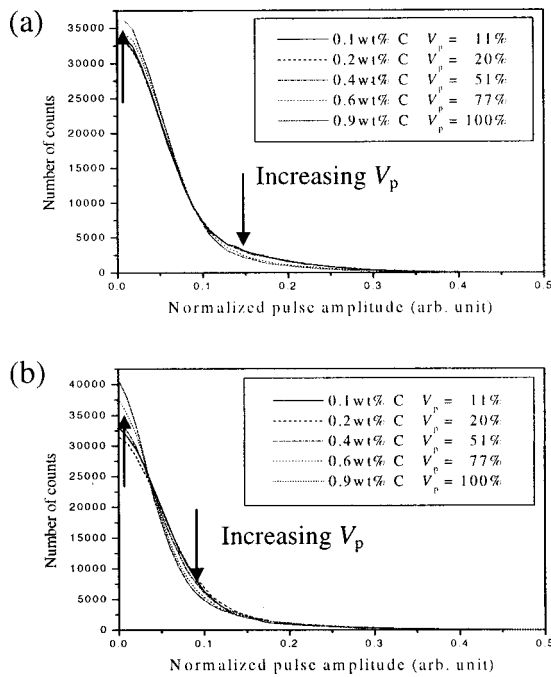


FIG. 2. Normalized pulse height distributions of the (a) experimental and (b) simulated BE signals of steel samples with various carbon contents.

for the initial increase in rms BE voltage. A definite trend was observed in the pulse height distributions of the experimental BE signals (Fig. 2) which show that increasing pearlite content results in a larger number of Barkhausen emissions of smaller amplitude. The rms BE voltage (Fig. 1) and pulse height distribution of the simulated BE signal (Fig. 2) exhibit dependence on the pearlite content similar to that observed in the experimental results.

In order to interpret the observed effect on the BE of varying pearlite content, theoretical simulations of BE signals were made using the hysteretic-stochastic model. Figure 3 shows the pulse height distributions of the BE signals simulated using various values of the correlation length parameter  $\xi$ . It is evident that decreasing  $\xi$  shifts the distribution of the simulated BE signals to smaller pulse amplitudes. Comparing the experimental and modeled results it can be concluded that increasing pearlite content reduces the range over which domain walls interact with pinning sites. This implies that in ferritic/pearlitic steels the displacement of a domain wall and hence the amplitude of the resulting BE jump become smaller with increasing pearlite content.

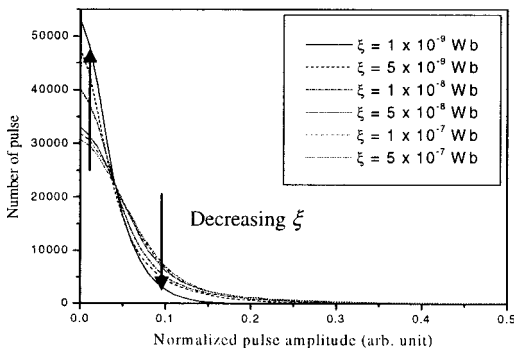


FIG. 3. Pulse height distributions of the BE signals simulated for the 0.6% C sample using various values of correlation length parameter  $\xi$ .

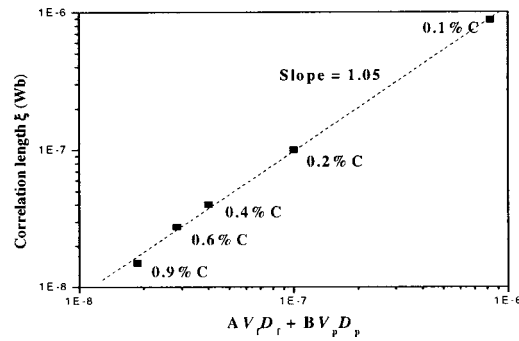


FIG. 4. The correlation length parameter  $\xi$  vs  $AV_jD_f + BV_pD_p$ .

The relation between the parameter  $\xi$  and the microstructure of the steel samples is shown in Fig. 4. The values of  $\xi$  were determined by obtaining the best fit of the simulated BE signal to the experimental data using a fixed value of  $1 \times 10^4 \text{ A}^2 \text{ m}^{-2} \text{ Wb}^{-1}$  for  $A$ . The effect of the parameter  $A$  on the BE signals was also investigated by performing a series of simulations using various values of  $A$  but fixed values of  $\xi$ . The results showed that the pulse height distributions of the simulated BE signals vary strongly with  $\xi$  but only weakly with  $A$  within the range of the parameters investigated in this study.

It is evident in Fig. 4 that the parameter  $\xi$  obeys the relation given in Eq. (5), suggesting that the correlation length of magnetization reversals is determined by the grain size of the majority phase (ferrite for  $<0.4\% \text{ C}$  and pearlite for  $>0.4\% \text{ C}$ ). The coefficients  $A$  and  $B$  were found to be  $6.19 \times 10^{-3} \text{ Wb m}^{-1}$  and  $1.44 \times 10^{-3} \text{ Wb m}^{-1}$ , respectively, by linear regression, indicating a larger contribution of ferrite to  $\xi$ . This can be explained by the fact that a domain wall can usually move over a larger distance in ferrite than in a colony of pearlite grains. In ferrite, once a domain wall is unpinned it can transverse several grains before it is pinned again at a grain boundary. On the other hand, a domain wall moving across a colony of pearlite grains can be easily pinned at a cementite lamella when it encounters a pearlite grain with the cementite lamellae lying parallel to the domain wall.

### ACKNOWLEDGMENTS

This work was supported by the NSF Industry/University Cooperative Research Program of the Center for Nondestructive Evaluation.

- <sup>1</sup>G. Bertotti, Phys. Rev. B **39**, 6737 (1989).
- <sup>2</sup>B. Alessandro, C. Beatrice, G. Bertotti, and A. Montorsi, J. Appl. Phys. **68**, 2901 (1990).
- <sup>3</sup>B. Alessandro, C. Beatrice, G. Bertotti, and A. Montorsi, J. Appl. Phys. **68**, 2908 (1990).
- <sup>4</sup>D. M. Clatterbuck, V. J. Garcia, M. J. Johnson, and D. C. Jiles, J. Appl. Phys. **87**, 4771 (2000).
- <sup>5</sup>D. C. Jiles, Czech. J. Phys. **50**, 893 (2000).
- <sup>6</sup>G. Bertotti and A. Montorsi, J. Magn. Magn. Mater. **83**, 214 (1990).
- <sup>7</sup>G. Bertotti, F. Fiorillo, and A. Montorsi, J. Appl. Phys. **67**, 5574 (1990).
- <sup>8</sup>D. C. Jiles and D. L. Atherton, J. Magn. Magn. Mater. **61**, 48 (1986).
- <sup>9</sup>M. Komatsubara and J. L. Porteseil, IEEE Trans. Magn. **23**, 3506 (1987).
- <sup>10</sup>M. G. Hetherington, J. P. Jakubovics, J. A. Szpunar, and B. K. Tanner, Philos. Mag. B **56**, 561 (1987).
- <sup>11</sup>B. Zhu, M. J. Johnson, C. C. H. Lo, and D. C. Jiles, IEEE Trans. Magn. **37**, 1095 (2001).
- <sup>12</sup>D. C. Jiles, J. B. Thielke, and M. K. Devine, IEEE Trans. Magn. **28**, 27 (1992).